International Journal of Innovative Computing, Information and Control
Volume **20**, Number **3**, June **2024**

ICIC International ©2024 ISSN 1349-4198
pp. 771–793

ANALYZING TRANSIENT RESPONSE VIBRATION IN WHEELCHAIR TRANSPORTATION: STATE SPACE MODELING FOR ENHANCED COMFORT AND WELL-BEING

Pongtep Weerapong[1,*], Kreetha Kaewkongtham[1], Narapong Chuaychai[1]
Chatchai Kaewdee[1], Weerayute Sudsomboon[1], Weeraphol Pansrinual[1]
Nghia Thi Mai[2], Mitsuki Katahira[3], Kotaro Hashikura[4]
Md Abdus Samad Kamal[4], Iwanori Murakami[4] and Kou Yamada[4]

[1]Faculty of Industrial Technology
Nakhon Si Thammarat Rajabhat University
M4 Tha-ngow Subdistrict, Maung District, Nakhon Si Thammarat 80280, Thailand
{ kreetha_kae; narapong_cho; chatchai_kae; weerayute_sud; weeraphol_pan }@nstru.ac.th
*Corresponding author: pongtap_wee@nstru.ac.th

[2]Department of Electrical and Electronic 1
Posts and Telecommunications Institute of Technology
Km10, Nguyen Trai, Ha Dong District, Hanoi 151090, Vietnam
nghiamt@ptit.edu.vn

[3]Graduate School of Science and Technology
[4]Division of Mechanical Science and Technology
Gunma University
1-5-1 Tenjincho, Kiryu 376-8515, Japan
{ t221b020; k-hashikura; maskamal; murakami; yamada }@gunma-u.ac.jp

Received October 2023; revised February 2024

Abstract. *Transient vibrations can affect the comfort and safety of wheelchair users. We developed and tested an 11-degree-of-freedom (11-DOF) model of a wheelchair-user system with foam-based cushions to examine the transient vibration effects on various body parts and the seat under sinusoidal inputs. We employed state space and Laplace transform methods to obtain analytical solutions for the displacement responses in the time domain. We validated our model with experimental data and achieved a high goodness-of-fit of 89.7[%]. We assessed the relative amplitude, frequency, and time of the maximum and minimum values of the displacement responses for different body segments and wheelchair components. We discovered that the torso was most affected by the vibrations, while the pelvis was least affected. We also noticed that the head was most stable and the abdomen was most unstable among the body segments. We calculated the strain value between the pelvis and abdomen and verified that it was below the critical level for potential damage to the body tissues. Our findings can assist in evaluating and enhancing the comfort and safety of wheelchair users during transient vibration events. They can also guide the design of systems that cater to the needs and preferences of wheelchair users and improve their quality of life. Furthermore, they can motivate future research on the vibration behavior of wheelchair-user systems, such as investigating different seating configurations, cushion materials and suspension systems within the 11-DOF model, considering other factors such as road surface conditions, wheel types and environmental factors, conducting user studies and collecting feedback on the proposed cushion designs and exploring the transmissibility behavior of seating systems and cushions with different input vibrations.*

Keywords: Transient response vibration, Mathematical model, State space analysis, Wheelchair-occupant systems, Vertical vibration dynamics

DOI: 10.24507/ijicic.20.03.771

1. **Introduction.** Wheelchair users experience vibrations from different sources, such as terrain, wheelchair components and user actions, that can affect their well-being and quality of life significantly. These vibrations can cause discomfort, pain, fatigue and trauma in different parts of the body [1, 2]. Manual wheelchair users are subject to vibrations that can harm their health, comfort and quality of life [3, 4, 5]. These vibrations are caused by non-periodic and abrupt excitations, such as propelling, braking and turning, which induce transient response vibrations in the wheelchair-user system [6, 7].

Transient response vibrations are the vibrations that arise when a system is subjected to a sudden change in its input or environment, such as a shock, impact or change in speed. They differ from steady state vibrations, which occur when a system attains a stable condition after a long time [8, 9, 10]. Transient response vibrations can induce large displacements, stresses and accelerations in the system, which may cause fatigue, pain, injury or trauma [11, 12]. Hence, it is vital to analyze and control the transient response vibrations in the wheelchair-occupant system to boost its performance and comfort. It is also imperative to develop effective techniques that diminish vibrations and improve user comfort during wheelchair transportation. In a wheelchair-occupant system, transient response vibrations can result from various factors, such as the terrain, wheelchair parts and user actions. For instance, when a wheelchair user encounters a bump, crashes into a curb or initiates or terminates wheelchair movement, transient response vibrations may occur. This vibration can negatively affect the health and comfort of wheelchair users, causing discomfort, pain, fatigue, and injury in different body parts. To alleviate transient response vibrations in wheelchair-occupant systems, various methods can be applied, such as altering wheelchair shape [1, 13, 14], selecting suitable engineering materials [15, 16, 17] and designing optimal cushions [8, 18, 19, 20]. These methods help to reduce vibrations and enhance user comfort during wheelchair transportation.

The paper by [9] advances the field by applying sophisticated modeling techniques to studying the vertical vibration dynamics of a wheelchair-occupant system. The paper showcases the expertise in biomechanics and human factors, especially in wheelchair ergonomics, that is necessary to understand the complex interaction between the human body and wheelchair systems. This refined modeling approach improves the paper's validity and reliability. Moreover, the paper collaborates with experts from various disciplines, such as biomechanics, vehicle dynamics and vibration analysis, to tackle the research problem from different perspectives and obtain insightful results. In line with the case, the paper uses frequency-domain solutions to solve the EOMs in multi-degree of freedom in matrix form of the complex Fourier transformation and constructs a composite model that integrates human and vehicle lumped-parameter models with multi-degree of freedom. The papers achieve remarkable accuracy in estimating vertical vibration behavior [21, 22]. These papers have significant practical implications because the researchers aim to reduce vibration response under low-cost economical by using seat cushion that can be used in the real world. They demonstrate their ability to transform research results into concrete solutions that can enhance the comfort and well-being of wheelchair users. It is vital to avoid health problems caused by vibrations, such as pain and damage to the muscles and bones. The researchers are committed to making effective cushions that can improve the lives of wheelchair users [1, 9, 23, 24]. They also follow user-centered design principles by studying how different parts of the body react to vibrations with actual cushions. This way, they account for the specific needs and comfort levels of wheelchair users, which makes the study more valid and shows its potential impact on enhancing the user experience [9, 24]. The results of this paper are expected to provide useful guidance for designing systems that suit the unique demands and preferences of wheelchair users [25, 26]. To further improve the field, the researchers suggest examining how different

seating arrangements, cushion materials, and suspension systems affect transient response vibration in the 11-DOF model. This shows their dedication to improving system design and increasing user comfort and safety [8, 9, 10].

Previous papers have examined the vibration responses of wheelchair-occupant systems under different conditions, such as road surfaces, wheelchair types and seat cushions. However, most of these researches focused on steady-state vibrations, which are consistent and periodic, and did not consider the transient nature of vibrations, which are more realistic and challenging to analyze. Moreover, most of these researches used numerical or experimental methods, which are limited by computational or practical constraints and did not provide analytical solutions, which are more general and comprehensive. To achieve a deeper comprehension of transient response vibration dynamics in the wheelchair-occupant system, this paper introduces a novel approach based on the state space methodology. This technique employs time as a fundamental dimension, encapsulating the system's evolution through a set of equations that depict the dynamic changes in system state variables over time [27]. The state space approach, a crucial element of our investigation, has unique capabilities. It excels in handling nonlinearities, uncertainties and disturbances inherent in complex systems. Furthermore, this methodology provides an elegant and effective framework for the design of feedback controllers and observers, adding a layer of sophistication to our analytical toolkit [28].

In this paper, we examine the transient vibration responses of a wheelchair-occupant system with foam-based seat cushions under sinusoidal vibration inputs, which are commonly used to simulate transient vibrations. We employ a state space model and Laplace transform to perform a time-domain analysis and derive analytical solutions for displacement responses. We validate our model with experimental data and investigate the effects of vibrations on the torso and pelvis, which have the largest relative displacements when seated on foam-based cushions. We classify the sinusoidal vibration inputs into low and high frequencies, based on their sources and activities. We determine potential damage thresholds based on peak to peak displacement of body parts and evaluate different foam-based cushions, providing practical guidance for choosing the most appropriate cushion for specific applications. This study is the first to investigate the transient vibration responses of a wheelchair-occupant system with foam-based seat cushions under sinusoidal vibration inputs and to establish potential damage thresholds based on peak to peak displacement of body parts. By describing the behavior of foam-based cushion under sinusoidal vibration inputs and defining potential damage thresholds [29, 30], we aim to improve the knowledge base for the selection and use of these cushions across various applications.

We propose a composite model of the wheelchair-occupant system and analyze its vibrational exposure. The paper is organized as follows. Section 2 discusses the challenges and previous works on wheelchair-occupant vibration analysis and provides the parameter values for the biodynamic and wheelchair models. Section 3 derives the equations of motion for the 11-DOF model, which accounts for the motion of the wheelchair and the occupant under sinusoidal excitation. Section 4 converts the equations of motion into matrix and state space forms, which are convenient for transient vibration analysis. Section 5 describes the solution method for the state space equations using Laplace transforms, and specifies the initial conditions by $x(0) = x_0$. The transient response is computed by applying the inverse Laplace transform to the state equation and solving for $y(t)$, considering the initial conditions. Section 6 validates the 11-DOF model with experimental data and analyzes the transient vibration responses and acceleration ratios of different components. Section 7 concludes the paper and highlights the main contributions and implications of this study.

2. **Analysis of Transient Vibration Response in Wheelchair-Occupant System.** Analyzing the transient vibration response of a wheelchair-occupant system presents unique challenges compared to studying the system in a steady state. The complex nature and diagnostic difficulties of the system make accurate analysis challenging, but it is possible to gain insights by examining its transient dynamics. In this paper, we shift the perspective from a steady state to the transient vibration response by considering the time-varying behavior of the system.

To facilitate the analysis, we begin by representing the occupant and the wheelchair as free-body diagrams (FBDs). This approach simplifies the solution of the linear system of ordinary differential equations in the 11-DOF model. By employing FBDs, we establish force equilibrium equations for each component in the system, enabling the derivation of the equations of motion. The system comprises 11 masses, 13 springs and 13 dampers and we analyze the forces acting on the system from a mechanical standpoint, including inertial forces, stiffness forces and damping forces. The interconnectivity between the masses is facilitated by the stiffness and damping forces, which generate reaction forces. To determine the direction of the forces, we construct FBDs for each component and apply Newton's third law of motion.

For instance, when considering masses m_{10} and m_{11}, respectively corresponding to the chassis and tire, with respect to the ground, the compressed rubber tire generates stiffness and damping forces that produce an upward thrust on the chassis and tire along the y-axis. The inertial forces of masses m_{10} and m_{11} oppose positional changes through their inertia. It is important to note that FBDs do not account for gravitational force or static displacement of each mass since they are in motion.

The objective of this investigation is to analyze the transient vibrational response of a person seated on a wheelchair during transportation. The seat cushion provides support to the lower body, while the upper segment lacks a backrest. The only external impulse received by the human body through the cushioned seat is a sinusoidal force input generated by the stiffness and damping forces from the wheelchair tires on the ground. External forces acting on the foot support of the wheelchair are disregarded in this paper, as their impact on vibration is minimal and primarily affects the trunk region of the body.

To analyze the transient response, we propose the occupant-wheelchair model as a mechanical system, as depicted in Figure 1. By employing the lumped-parameter model, we can design the system to examine the transient response within a low frequency range of 0.5∼11 [Hz]. The 11-block composite model, known as the 11-DOF model, consists of a wheelchair model and a human occupant model interconnected through stiffness and damping constants. The blocks represent masses denoted as m_i with $i = 1, 2, \ldots, 11$, corresponding to various body parts such as the head, pelvis, seat, suspension, tire and others. The stiffness and damping constants denoted as k_i and c_i respectively, establish connections between these blocks. Detailed parameter values for the body parts and wheelchair components can be found in Tables 1 and 2. Subsequent sections will discuss further analysis details using a 2-D sagittal plane perspective, as depicted in Figure 1.

This paper presents a novel and rigorous analysis of the transient vibration response in wheelchair-occupant systems. By incorporating empirical data, the simulation achieves higher accuracy, providing a more realistic representation of the system's behavior. The occupant is modeled as a 7-DOF system, comprising seven masses: m_1 for the head, m_2 for the back (including neck), m_3 for the torso (including shoulders), m_4 for the thorax (including lungs), m_5 for the diaphragm (including stomach), m_6 for the abdomen (including intestines) and m_7 for the pelvis (including hips). The tissue between the torso and back exhibits viscoelastic behavior, which is characterized by the damping coefficient c_{32} and the spring constant k_{32}. Table 1 details the parameter values governing these

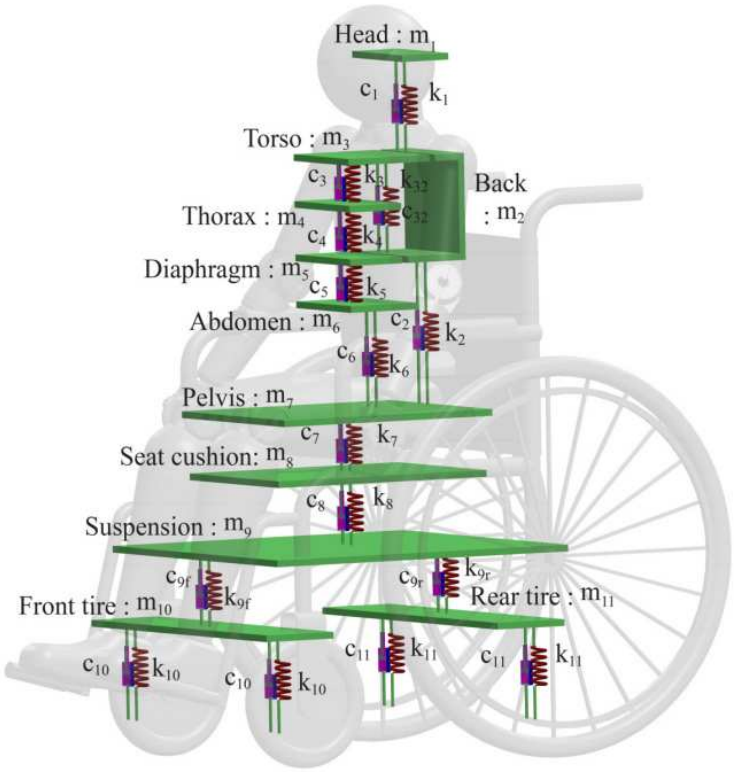

FIGURE 1. Free-body diagrams (FBDs) of the lumped-parameter model for the wheelchair-occupant system

TABLE 1. Parameter values for the biodynamic model [30, 31]

Mass $[M]$ [kg]	Damping constant $[C]$ [N/m/sec]	Spring constant $[K]$ [N/m]
$m_7 = 27.7$	$c_7 = 378$	$k_7 = 25500$
$m_6 = 6.02$	$c_6 = 298$	$k_6 = 894.1$
$m_5 = 0.46$	$c_5 = 298$	$k_5 = 894.1$
$m_4 = 1.38$	$c_4 = 298$	$k_4 = 894.1$
$m_3 = 33.33$	$c_3 = 298$	$k_3 = 894.1$
	$c_{32} = 3651$	$k_{32} = 53640$
$m_2 = 6.94$	$c_2 = 3651$	$k_2 = 53640$
$m_1 = 5.5$	$c_1 = 3651$	$k_1 = 53640$

TABLE 2. Parameter values for the manual wheelchair model [8, 32]

Mass $[M]$ [kg]	Damping constant $[C]$ [N/m/sec]	Spring constant $[K]$ [N/m]
$m_{11} = 1.6$	$c_{11} = 500$	$k_{11} = 6000$
$m_{10} = 1.0$	$c_{10} = 500$	$k_{10} = 60000$
$m_9 = 15$	$c_{9f} = 700$	$k_{9f} = 13400$
	$c_{9r} = 700$	$k_{9r} = 74600$
$m_8 = 1.5$	$c_8 = 1689$	$k_8 = 183200$
vibration input magnitude, $y_0 = 5.0$ [mm].		

The parameter value for each suspension is marked by a subscript: f for the front and r for the rear.

interconnections, derived from comprehensive studies on anatomical subsystems. The occupant's lower body is supported by the seat cushion (m_8), while the upper body has no backrest. The wheelchair is modeled as a 4-DOF system, comprising four masses: m_8 for the seat cushion, m_9 for the suspension, m_{10} for the front tires and m_{11} for the rear tires. The suspension is rigidly attached to both pairs of tires. The front and rear tires are assumed to have identical mass, stiffness and damping values. Table 2 details the parameter values governing these interconnections, derived from comprehensive studies on wheelchair subsystems. This analysis represents a significant advancement in understanding the complex dynamics exhibited by wheelchair-occupant systems. By utilizing synthetic modeling techniques, providing disruptive insights, and adopting a comprehensive approach, the paper contributes valuable knowledge to the field. It deepens our understanding of the system's behavior under diverse conditions, paving the way for improved design considerations and interventions that enhance overall performance and user comfort.

3. **Derivation and Analysis of Equations of Motion of the Eleven DOFs.** In this section, we present the equations of motion for an 11-DOF model of a wheelchair-occupant system. This model describes the motion of a wheelchair and the occupant sitting on it. The mass matrix, denoted by $[M]$, represents the inertia of the system and is an 11×11 diagonal matrix. Each diagonal element corresponds to the mass of a specific component in the system, ranging from m_1 to m_{11}. The mass matrix relates the accelerations (second time derivatives) of the displacements (y_1 to y_{11}). The damping matrix, denoted by $[C]$, is an 11×11 matrix that accounts for the damping forces in the system. Each element (c_{ij}) represents the damping coefficient between the i-th and j-th displacements. The damping matrix relates the velocities (first time derivatives) of the displacements ($\dot{y}_1$ to $\dot{y}_{11}$). Damping opposes the motion and dissipates energy. The stiffness matrix, denoted by $[K]$, is also an 11×11 matrix. Each element (k_{ij}) represents the stiffness coefficient between the i-th and j-th displacements. The stiffness matrix relates the displacements (y_1 to y_{11}) and determines how the system responds to external forces, influencing the magnitude and direction of displacements.

The right-hand side of the equations represents the external forces acting on the system. Specifically, we have two non-zero elements (k_{10} and k_{11}) multiplied by the vector of initial displacements (y_0) and transposed. This term represents an external force applied to specific displacements. Similarly, we have two non-zero elements (c_{10} and c_{11}) multiplied by the vector of initial velocities ($\dot{y}_0$) and transposed. This term represents an external force applied to specific velocities. By solving these equations, we can determine the accelerations ($\ddot{y}_1$ to $\ddot{y}_{11}$) of the displacements, which describe the motion of the wheelchair-occupant system over time. Overall, this mathematical model provides a quantitative representation of the 11-DOF wheelchair-occupant system, considering mass, damping, stiffness, and external forces. It is useful for analyzing, simulating, and controlling the system's motion.

3.1. **Sinusoidal excitation analysis of the 11-DOF wheelchair-occupant system.** In this subsection, we analyze the response of the 11-DOF wheelchair-occupant system to sinusoidal excitation from the road surface. The DOFs in the system include the vertical displacements of the front and rear tires, the seat, the backrest, and the head, neck, thorax, lumbar, pelvis, and thigh of the occupant. The road surface excitation is modeled as a sinusoidal force with frequency ω.

To derive the equations of motion for the system, we use the following notation: $[M]$, $[C]$, and $[K]$ are the 11×11 mass, damping, and stiffness matrices of the system,

respectively. They are composed of the mass, damping and stiffness coefficients of each component, such as m_i, c_i and k_i, where i is the index of the component. The displacement, velocity and acceleration vectors of the system are represented by $y(t)$, $\dot{y}(t)$ and $\ddot{y}(t)$, respectively. These vectors contain the DOFs of each component, such as $y_i(t)$, $\dot{y}_i(t)$ and $\ddot{y}_i(t)$. The force vector of the external excitation is denoted by $F(t)$. It depends on the displacement and velocity vectors of the road surface, $y_0(t)$ and $\dot{y}_0(t)$, as well as the damping and stiffness coefficients of the contact between the tires and the road surface, namely c_{10}, c_{11}, k_{10} and k_{11}. Using these notations, we can write the equations of motion for the system in matrix form as

$$[M]\{\ddot{y}(t)\} + [C]\{\dot{y}(t)\} + [K]\{y(t)\} = \{F(t)\}, \tag{1}$$

$$\{F(t)\} = [c_{10} + c_{11}]\{y_0(t)\ \omega\cos\omega t\} + [k_{10} + k_{11}]\{y_0(t)\sin\omega t\}, \tag{2}$$

where $[M]$, $[C]$ and $[K]$ are 11×11 mass, damping and stiffness matrices, respectively; $\{y(t)\}$, $\{\dot{y}(t)\}$ and $\{\ddot{y}(t)\}$ are displacement, velocity and acceleration vector of the response system; $\{F(t)\}$ is the force vectors of the external excitation; $\{y_0(t)\}$ is the displacement vector of the external excitation system.

3.2. **Equations of motion for the 11-DOF wheelchair-occupant model.** This section presents the system of equations of motion for an 11-DOF wheelchair-occupant model. The model comprises various masses representing different components, including the head, back, torso, thorax, diaphragm, abdomen, pelvis, seat cushion, suspension, front tires, and rear tires. The governing equations describe the dynamics of these masses, accounting for their inertial properties and the forces exerted on them by stiffness and damping elements. The equations of motion are derived by applying force equilibrium principles to the human body and wheelchair mass. The resulting second-order linear ordinary differential equations represent the motion of each mass in terms of its acceleration, velocity, and displacement. Solving these equations yields a set of 11 equations that describe the model's 11-DOFs.

The governing EOM for each mass comprises its inertia term and forces exerted on it by stiffnesses and dampers due to the relative motion of connected masses. In an EOM, variables such as m_i, k_i, c_i, y_i, $\dot{y}_i$ and $\ddot{y}_i$, $(i = 1, 2, \ldots, 11)$ represent components such as rear tires, front tires, suspension, seat cushion, pelvis, abdomen, diaphragm, thorax, torso, back and head. y_0 and $\dot{y}_0$ signify corresponding displacements and velocities upon excitation. The governing second-order linear ordinary differential equations of the nine masses of the composite model (shown in Figure 1) are derived from the FBD by applying force equilibrium principles to the human body and wheelchair mass. After mathematical adjustment according to our literature review [21, 22], the EOMs are transformed into linear polynomials – altogether eleven equations to describe the model's eleven DOFs. From the FBDs shown in Figure 1, eleven EOMs are obtained by solving Equations (3) to (13). The EOMs are summarized as follows.

1. The head

$$\ddot{y}_1 = \frac{c_1(\dot{y}_2 - \dot{y}_1) + k_1(y_2 - y_1)}{m_1}, \tag{3}$$

where m_1, c_1, k_1, $\ddot{y}_1$, $\dot{y}_1$ and y_1 are the mass, damping, spring, acceleration, velocity and displacement of the head. $\dot{y}_2$ and y_2 are, respectively, the velocity and displacement of the back.

2. The back

$$\ddot{y}_2 = \frac{c_1(\dot{y}_1 - \dot{y}_2) + c_{32}(\dot{y}_3 - \dot{y}_2) + c_2(\dot{y}_3 - \dot{y}_2) + k_1(y_1 - y_2) + k_2(y_3 - y_2) + k_{32}(y_3 - y_2)}{m_2}, \tag{4}$$

where (i) m_2, c_2, k_2, $\ddot{y}_2$, $\dot{y}_2$ and y_2 are the mass, damping, spring, acceleration, velocity and displacement of the back, (ii) c_{32}, k_{32} are, respectively, the damping and spring constant of tissue between the torso and back, and (iii) $\dot{y}_3$, y_3 refer to the velocity and displacement of the torso, respectively.

3. The torso

$$\ddot{y}_3 = \frac{c_{32}(\dot{y}_2 - \dot{y}_3) + c_3(\dot{y}_4 - \dot{y}_3) + k_{32}(y_2 - y_3) + k_3(y_4 - y_3)}{m_3}, \tag{5}$$

where (i) m_3, c_3, k_3, and $\ddot{y}_3$ are the mass, damping, spring, and acceleration of the torso, and (ii) $\dot{y}_4$, y_4 refer to the velocity and displacement of the thorax, respectively.

4. The thorax

$$\ddot{y}_4 = \frac{c_3(\dot{y}_3 - \dot{y}_4) + c_4(\dot{y}_5 - \dot{y}_4) + k_3(y_3 - y_4) + k_4(y_5 - y_4)}{m_4}, \tag{6}$$

where (i) m_4, c_4, k_4, and $\ddot{y}_4$ are the mass, damping, spring, and acceleration of the thorax, and (ii) $\dot{y}_5$, y_5 refer to the velocity and displacement of the diaphragm, respectively.

5. The diaphragm

$$\ddot{y}_5 = \frac{c_4(\dot{y}_4 - \dot{y}_5) + c_5(\dot{y}_6 - \dot{y}_5) + k_4(y_4 - y_5) + k_5(y_6 - y_5)}{m_5}, \tag{7}$$

where (i) m_5, c_5, k_5, and $\ddot{y}_5$ are the mass, damping, spring, and acceleration of the diaphragm, and (ii) $\dot{y}_6$, y_6 refer to the velocity and displacement of the abdomen, respectively.

6. The abdomen

$$\ddot{y}_6 = \frac{c_5(\dot{y}_5 - \dot{y}_6) + c_6(\dot{y}_7 - \dot{y}_6) + k_5(y_5 - y_6) + k_6(y_7 - y_6)}{m_6}, \tag{8}$$

where (i) m_6, c_6, k_6, and $\ddot{y}_6$ are the mass, damping, spring, and acceleration of the abdomen, and (ii) $\dot{y}_7$, y_7 refer to the velocity and displacement of the pelvis, respectively.

7. The pelvis

$$\ddot{y}_7 = \frac{c_6(\dot{y}_6 - \dot{y}_7) + c_7(\dot{y}_2 - \dot{y}_7) + c_2(\dot{y}_2 - \dot{y}_7) + k_6(y_6 - y_7) + k_7(y_2 - y_7) + k_2(y_2 - y_7)}{m_7}, \tag{9}$$

where (i) m_7, c_7, k_7, and $\ddot{y}_7$ are the mass, damping, spring, and acceleration of the abdomen, and (ii) $\dot{y}_8$, y_8 refer to the velocity and displacement of the seat cushion, respectively.

8. The seat cushion

$$\ddot{y}_8 = \frac{c_7(\dot{y}_7 - \dot{y}_8) + c_8(\dot{y}_9 - \dot{y}_8) + k_7(y_7 - y_8) + k_8(y_9 - y_8)}{m_8}, \tag{10}$$

where (i) m_8, c_8, k_8, and $\ddot{y}_8$ are the mass, damping, spring, and acceleration of the seat cushion, and (ii) $\dot{y}_9$, y_9 refer to the velocity and displacement of the suspension, respectively.

9. The suspension

$$\ddot{y}_9 = \frac{c_8(\dot{y}_8 - \dot{y}_9) + c_{9f}(\dot{y}_{10} - \dot{y}_9) + c_{9r}(\dot{y}_{11} - \dot{y}_9) + k_{9r}(y_{11} - y_9) + k_{9f}(y_{10} - y_9) + k_8(y_8 - y_9)}{m_9}, \tag{11}$$

where (i) m_9, c_{9r}, and k_{9r} are the mass, damping, spring of the rear suspension, (ii) c_{9f} and k_{9f} are damping and spring of the front suspension, (iii) $\ddot{y}_9$ is acceleration of the suspension, and (iv) $\dot{y}_{10}$ and y_{10} refer to the velocity and displacement of the front tires, respectively and (v) $\dot{y}_{11}$ and y_{11} refer to the velocity and displacement of the rear tires, respectively

10. The front tires

$$\ddot{y}_{10} = \frac{c_{9f}(\dot{y}_9 - \dot{y}_{10}) + c_{10}(\dot{y}_0 - \dot{y}_{10}) + k_{9f}(y_9 - y_{10}) + k_{10}(y_0 - y_{10}) + c_{10}y_0\omega\cos\omega t + k_{10}y_0\sin\omega t}{m_{10}} \quad (12)$$

where (i) m_{10} is the mass of the front tires, (ii) $\ddot{y}_{10}$ refers to acceleration of the tires, (ii) c_{10} and k_{10} are, respectively, the damping and spring constant of front tires, (iii) $\dot{y}_0$ and y_0 refer, respectively, to the input velocity and displacement of the tires contact points to the floor. The floor surface will cause the tires to compress, and (iv) y_0, ω are, respectively, the amplitude of input displacement excitation and circular frequency of this displacement applied at the tire contact points to the floor.

11. The rear tires

$$\ddot{y}_{11} = \frac{c_{9r}(\dot{y}_9 - \dot{y}_{11}) + c_{11}(\dot{y}_0 - \dot{y}_{11}) + k_{9r}(y_9 - y_{11}) + k_{11}(y_0 - y_{11}) + c_{11}y_0\omega\cos\omega t + k_{11}y_0\sin\omega t}{m_{11}}, \quad (13)$$

where (i) m_{11} is the mass of the rear tires, (ii) $\ddot{y}_{11}$ refers to acceleration of the rear tires, and (iii) c_{11} and k_{11} are, respectively, the damping and spring constant of rear tires. These equations of motion describe the dynamic behavior of each component in the 11-DOF wheelchair-occupant model. By considering the interplay of damping, spring constants, displacements, and velocities of adjacent components, these equations provide a comprehensive representation of the system's dynamics. Analyzing and solving these equations allow for a deeper understanding of the wheelchair-occupant interaction and can aid in designing and optimizing wheelchair systems for improved comfort and stability. These equations of motion provide a detailed description of the dynamics of each component in the wheelchair-occupant model. By considering the effects of damping, spring constants, displacements, velocities, and external excitation, these equations allow for a comprehensive analysis of the system's behavior. They are essential for studying and optimizing wheelchair designs to ensure comfort, stability, and overall performance for the occupant.

4. State Space Form for Transient Response Vibration Analysis.

The equations of motion for transient response vibration analysis can be expressed using the state space form and matrix notation. The state-space representation consists of two equations: the state equation and the output equation. The state equation describes the change of the system state over time as a function of the system input. The output equation describes the dependence of the system output on the system state and the system input.

4.1. State equation of the system.

We derive the state equation of the system, which is a convenient and compact way to express the equations of motion for transient response vibration analysis. The state equation describes how the state of the system changes over time as a function of the system input. The state equation is given by

$$\dot{x}(t) = [A]x(t) + [B]u(t). \quad (14)$$

Here, the column vector x represents the system's state, which includes the displacements and velocities of different body segments. The scalar u denotes the system input, which is the transient force applied to the system. The matrix A represents the system matrix, which contains the stiffness and damping coefficients of the system. The matrix B represents the input matrix, which indicates how the input affects each state variable. The input matrix B can be modified depending on the input scenario. In a system with 11-DOF where transient forces are applied to mass 10 and mass 11, the matrix B has non-zero elements in the corresponding rows. In the next subsection, we will discuss how to obtain the system output using the output equation.

4.2. **Output equation in state-space representation.** We derive the system output, which is the response of the system to the transient input, using the state-space representation. The input matrix B has identical elements in those rows for multiple degrees of freedom experiencing the same transient force u, with sinusoidal forces having amplitudes proportional to y_0 applied to mass 10 and mass 11. To obtain the system output, we introduce an output matrix C to relate the outputs to the states. We also introduce a direct transmission matrix D, which accounts for outputs that directly depend on the inputs, without involving the states. The output equation is given by

$$y = [C]x(t) + [D]u(t). \tag{15}$$

The output matrix C has a number of rows equal to the number of outputs, and a number of columns equal to the number of states. The direct transmission matrix D has the same number of rows as the output matrix C and the same number of columns as the input matrix B [33, 34]. In the next subsection, we will discuss how to solve the output equation using Laplace transform.

5. **Solving EOMs in State Space Form Using Laplace Transforms.** Solving equations of motion (EOMs) in state space form involves using Laplace transforms and starting with the complete set of state space equations. Here, the initial conditions are set by $x(0) = x_0$. To solve for the transient response, we take the matrix Laplace transform of the state equation and solve for $x(s)$, taking account of the initial conditions.

5.1. **Matrix notation for state variables and derivatives.** We use the following variables to denote the state variables and their derivatives:

$$\begin{cases} x_1 = y_1 \text{ displacement of mass 1} \\ x_2 = \dot{y}_1 \text{ velocity of mass 1} \\ x_3 = y_2 \text{ displacement of mass 2} \\ x_4 = \dot{y}_2 \text{ velocity of mass 2} \\ x_5 = y_3 \text{ displacement of mass 3} \\ x_6 = \dot{y}_3 \text{ velocity of mass 3} \\ x_7 = y_4 \text{ displacement of mass 4} \\ x_8 = \dot{y}_4 \text{ velocity of mass 4} \\ x_9 = y_5 \text{ displacement of mass 5} \\ x_{10} = \dot{y}_5 \text{ velocity of mass 5} \\ x_{11} = y_6 \text{ displacement of mass 6} \\ x_{12} = \dot{y}_6 \text{ velocity of mass 6} \\ x_{13} = y_7 \text{ displacement of mass 7} \\ x_{14} = \dot{y}_7 \text{ velocity of mass 7} \\ x_{15} = y_8 \text{ displacement of mass 8} \\ x_{16} = \dot{y}_8 \text{ velocity of mass 8} \end{cases} \tag{16}$$

$$\begin{cases} x_{17} = y_9 \text{ displacement of mass 9} \\ x_{18} = \dot{y}_9 \text{ velocity of mass 9} \\ x_{19} = y_{10} \text{ displacement of mass 10} \\ x_{20} = \dot{y}_{10} \text{ velocity of mass 10} \\ x_{21} = y_{11} \text{ displacement of mass 11} \\ x_{22} = \dot{y}_{11} \text{ velocity of mass 11} \end{cases} \tag{17}$$

5.2. **Laplace transforms for state space analysis with initial conditions.**

5.2.1. *Applying Laplace transforms to linear ordinary differential equations (LODEs) with initial conditions.* In our previous discussion, we explored the application of Laplace transforms to LODEs with zero initial conditions. However, when considering the transient response of a system governed by LODEs with non-zero initial conditions, the initial conditions become important. In such cases, we use the basic definition of the differentiation operation to obtain the Laplace transform of first and second-order differential equations with initial conditions $\{x(0)\}$ and $\{\dot{x}(0)\}$. Taking the matrix Laplace transform of a first-order differential equation with initial conditions:

$$\mathscr{L}\{x(t)\} = \{x(s)\}, \tag{18}$$

$$\mathscr{L}\{\dot{x}(t)\} = s\{x(s)\} - \{x(0)\}. \tag{19}$$

By taking the Laplace transform of the Equation (16):

$$\mathscr{L}\{\dot{x}(t)\} = \mathscr{L}[A]\{x(t)\} + \mathscr{L}[B]u(t), \tag{20}$$

and simplifying, we obtain

$$s\{x(s)\} - \{x(0)\} = [A]\mathscr{L}\{x(s)\} + [B]\mathscr{L}\{u(s)\} = [A]\{x(s)\} + [B]u(s), \tag{21}$$

$$(sI - [A])\{x(s)\} = \{x(0)\} + [B]u(s), \tag{22}$$

$$\{x(s)\} = (sI - [A])^{-1}\{x(0)\} + (sI - [A])^{-1}[B]u(s), \tag{23}$$

solving for the output vector $y(s)$:

$$\{y(s)\} = [C]\{x(s)\}, \tag{24}$$

$$\{y(s)\} = [C](sI - [A])^{-1}\{x(0)\} + [C](sI - [A])^{-1}\{x(0)\}[B]u(s). \tag{25}$$

The input matrix B and output matrix C are the same as in the previous state space formulations. There is a new term in the equation for the Laplace transform of $\{y(s)\}$, the term $(s[I] - [A])^{-1}$. There are many methods of calculating the inverse $(s[I] - [A])^{-1}$ [34]. Then $\{y(s)\}$ can be back-transformed term by term to get the solution in the time domain, as we will see in the next section.

$$(s[I] - [A])^{-1} = \frac{[I]}{s} + \frac{[A]^n}{s^{n+1}}, \ (n = 1, 2, \ldots). \tag{26}$$

5.3. **Solving EOMs using inverse matrix Laplace transform and matrix exponential.** Now that we have the inverse in series form, it is easy to back-transform to the time domain, term by term. The inverse Laplace transform of $(s[I] - [A])^{-1}$ is denoted by $e^{[A]t}$, representing the matrix exponential as indicated in (27):

$$\mathscr{L}^{-1}\left\{(s[I] - [A])^{-1}\right\} = e^{[A]t}. \tag{27}$$

Using the matrix exponential, we can back-transform the entire equation of motion, from (22)

$$\mathscr{L}^{-1}\{x(s)\} = \mathscr{L}^{-1}\left[(s[I] - [A])^{-1}\{x(0)\} + (s[I] - [A])^{-1}[B]u(s)\right]. \tag{28}$$

The result is

$$\{x(t)\} = e^{[A]t}\{x(0)\} + \int_0^t e^{[A](t-\tau)}[B]u(\tau)d(\tau). \tag{29}$$

The first term in (28) is the response due to the initial condition of the state and the second term is the response due to the input. The second term is the convolution integral, which arises from back-transforming the product of two Laplace transforms. Using the series form of the inverse, we can easily back-transform each term to the time domain:

$$\mathscr{L}^{-1}\{y(s)\} = [C]\mathscr{L}^{-1}\{x(s)\}. \tag{30}$$

The output equation for the displacement outputs:

$$\{y(t)\} = [C]\{x(t)\} = [C]e^{[A]t}\{x(0)\} + \int_0^t e^{[A](t-\tau)}[B]u(\tau)d(\tau). \tag{31}$$

The following system dynamics can be represented by rewriting the equations above in matrix form as: $sI - A$

$$[sI - A]$$

$$= \begin{bmatrix}
s & -1 & 0 & 0 & 0 & 0 & 0 & 0 & 0 & 0 & 0 & 0 & 0 & 0 & 0 & 0 & 0 & 0 & 0 & 0 & 0 & 0 \\
I_{01} & I_{02} & I_{03} & I_{04} & 0 & 0 & 0 & 0 & 0 & 0 & 0 & 0 & 0 & 0 & 0 & 0 & 0 & 0 & 0 & 0 & 0 & 0 \\
0 & 0 & s & -1 & 0 & 0 & 0 & 0 & 0 & 0 & 0 & 0 & 0 & 0 & 0 & 0 & 0 & 0 & 0 & 0 & 0 & 0 \\
I_{05} & I_{06} & I_{07} & I_{08} & I_{09} & I_{10} & 0 & 0 & 0 & 0 & 0 & 0 & I_{11} & I_{12} & 0 & 0 & 0 & 0 & 0 & 0 & 0 & 0 \\
0 & 0 & 0 & 0 & s & -1 & 0 & 0 & 0 & 0 & 0 & 0 & 0 & 0 & 0 & 0 & 0 & 0 & 0 & 0 & 0 & 0 \\
0 & 0 & I_{13} & I_{14} & I_{15} & I_{16} & I_{17} & I_{18} & 0 & 0 & 0 & 0 & 0 & 0 & 0 & 0 & 0 & 0 & 0 & 0 & 0 & 0 \\
0 & 0 & 0 & 0 & 0 & 0 & s & -1 & 0 & 0 & 0 & 0 & 0 & 0 & 0 & 0 & 0 & 0 & 0 & 0 & 0 & 0 \\
0 & 0 & 0 & 0 & I_{19} & I_{20} & I_{21} & I_{22} & I_{23} & I_{24} & 0 & 0 & 0 & 0 & 0 & 0 & 0 & 0 & 0 & 0 & 0 & 0 \\
0 & 0 & 0 & 0 & 0 & 0 & 0 & 0 & s & -1 & 0 & 0 & 0 & 0 & 0 & 0 & 0 & 0 & 0 & 0 & 0 & 0 \\
0 & 0 & 0 & 0 & 0 & 0 & I_{25} & I_{26} & I_{27} & I_{28} & I_{29} & I_{30} & 0 & 0 & 0 & 0 & 0 & 0 & 0 & 0 & 0 & 0 \\
0 & 0 & 0 & 0 & 0 & 0 & 0 & 0 & 0 & 0 & s & -1 & 0 & 0 & 0 & 0 & 0 & 0 & 0 & 0 & 0 & 0 \\
0 & 0 & 0 & 0 & 0 & 0 & 0 & 0 & I_{31} & I_{32} & I_{33} & I_{34} & I_{35} & I_{36} & 0 & 0 & 0 & 0 & 0 & 0 & 0 & 0 \\
0 & 0 & 0 & 0 & 0 & 0 & 0 & 0 & 0 & 0 & 0 & 0 & s & -1 & 0 & 0 & 0 & 0 & 0 & 0 & 0 & 0 \\
0 & 0 & I_{37} & I_{38} & 0 & 0 & 0 & 0 & 0 & 0 & I_{39} & I_{40} & I_{41} & I_{42} & I_{43} & I_{44} & 0 & 0 & 0 & 0 & 0 & 0 \\
0 & 0 & 0 & 0 & 0 & 0 & 0 & 0 & 0 & 0 & 0 & 0 & 0 & 0 & s & -1 & 0 & 0 & 0 & 0 & 0 & 0 \\
0 & 0 & 0 & 0 & 0 & 0 & 0 & 0 & 0 & 0 & 0 & 0 & I_{45} & I_{46} & I_{47} & I_{48} & I_{49} & I_{50} & 0 & 0 & 0 & 0 \\
0 & 0 & 0 & 0 & 0 & 0 & 0 & 0 & 0 & 0 & 0 & 0 & 0 & 0 & 0 & 0 & s & -1 & 0 & 0 & 0 & 0 \\
0 & 0 & 0 & 0 & 0 & 0 & 0 & 0 & 0 & 0 & 0 & 0 & 0 & 0 & I_{51} & I_{52} & I_{53} & I_{54} & I_{55} & I_{56} & I_{57} & I_{58} \\
0 & 0 & 0 & 0 & 0 & 0 & 0 & 0 & 0 & 0 & 0 & 0 & 0 & 0 & 0 & 0 & 0 & 0 & s & -1 & 0 & 0 \\
0 & 0 & 0 & 0 & 0 & 0 & 0 & 0 & 0 & 0 & 0 & 0 & 0 & 0 & 0 & 0 & I_{59} & I_{60} & I_{61} & I_{62} & 0 & 0 \\
0 & 0 & 0 & 0 & 0 & 0 & 0 & 0 & 0 & 0 & 0 & 0 & 0 & 0 & 0 & 0 & 0 & 0 & 0 & 0 & s & -1 \\
0 & 0 & 0 & 0 & 0 & 0 & 0 & 0 & 0 & 0 & 0 & 0 & 0 & 0 & 0 & 0 & I_{63} & I_{64} & 0 & 0 & I_{65} & I_{66}
\end{bmatrix} \tag{32}$$

$I_{01} = \frac{k_1}{m_1}$; $I_{02} = \frac{s+c_1}{m_1}$; $I_{03} = -\frac{k_1}{m_1}$; $I_{04} = -\frac{c_1}{m_1}$; $I_{05} = -\frac{k_1}{m_2}$; $I_{06} = -\frac{c_1}{m_2}$; $I_{07} = \frac{k_1+k_2+k_{32}}{m_2}$; $I_{08} = \frac{s+(c_1+c_2+c_{32})}{m_2}$; $I_{09} = -\frac{k_{32}}{m_2}$; $I_{10} = -\frac{c_{32}}{m_2}$; $I_{11} = -\frac{k_2}{m_2}$; $I_{12} = -\frac{c_2}{m_2}$; $I_{13} = -\frac{k_{32}}{m_3}$; $I_{14} = -\frac{c_{32}}{m_3}$; $I_{15} = \frac{k_3+k_{32}}{m_3}$; $I_{16} = \frac{s+(c_3+c_{32})}{m_3}$; $I_{17} = -\frac{k_3}{m_3}$; $I_{18} = -\frac{c_3}{m_3}$; $I_{19} = -\frac{k_3}{m_4}$; $I_{20} = -\frac{c_3}{m_4}$; $I_{21} = \frac{k_3+k_4}{m_4}$; $I_{22} = \frac{s+(c_3+c_4)}{m_4}$; $I_{23} = -\frac{k_4}{m_4}$; $I_{24} = -\frac{c_4}{m_4}$; $I_{25} = -\frac{k_4}{m_5}$; $I_{26} = -\frac{c_4}{m_5}$; $I_{27} = \frac{k_4+k_5}{m_5}$; $I_{28} = \frac{s+(c_4+c_5)}{m_5}$; $I_{29} = -\frac{k_5}{m_5}$; $I_{30} = -\frac{c_5}{m_5}$; $I_{31} = -\frac{k_5}{m_6}$; $I_{32} = -\frac{c_5}{m_6}$; $I_{33} = \frac{(k_5+k_6)}{m_6}$; $I_{34} = \frac{s+(c_5+c_6)}{m_6}$; $I_{35} = -\frac{k_6}{m_6}$; $I_{36} = -\frac{c_6}{m_6}$; $I_{37} = -\frac{k_2}{m_7}$; $I_{38} = -\frac{c_2}{m_7}$; $I_{39} = -\frac{k_6}{m_7}$; $I_{40} = -\frac{c_6}{m_7}$; $I_{41} = \frac{(k_2+k_6+k_7)}{m_7}$; $I_{42} = \frac{s+(c_2+c_6+c_7)}{m_7}$; $I_{43} = -\frac{k_7}{m_7}$; $I_{44} = -\frac{c_7}{m_7}$; $I_{45} = -\frac{k_7}{m_8}$; $I_{46} = -\frac{c_7}{m_8}$; $I_{47} = \frac{k_7+k_8}{m_8}$; $I_{48} = \frac{s+(c_7+c_8)}{m_8}$; $I_{49} = -\frac{k_8}{m_8}$; $I_{50} = -\frac{c_8}{m_8}$; $I_{51} = -\frac{k_8}{m_9}$; $I_{52} = -\frac{c_8}{m_9}$; $I_{53} = \frac{(k_8+k_{9f}+k_{9r})}{m_9}$; $I_{54} = \frac{s+(c_8+c_{9f}+c_{9r})}{m_9}$; $I_{55} = -\frac{k_{9f}}{m_9}$; $I_{56} = -\frac{c_{9f}}{m_9}$; $I_{57} = -\frac{k_{9r}}{m_9}$; $I_{58} = -\frac{c_{9r}}{m_9}$; $I_{59} = -\frac{k_{9f}}{m_{10}}$; $I_{60} = -\frac{c_{9f}}{m_{10}}$; $I_{61} = \frac{k_{10}+k_{9f}}{m_{10}}$; $I_{62} = \frac{s+(c_{10}+c_{9f})}{m_{10}}$; $I_{63} = -\frac{k_{9r}}{m_{11}}$; $I_{64} = -\frac{c_{9r}}{m_{11}}$; $I_{65} = \frac{k_{11}+k_{9r}}{m_{11}}$; $I_{66} = \frac{s+(c_{11}+c_{9r})}{m_{11}}$.

The output equation, which solely accounts for displacement outputs and excludes velocities without a feed-through term, is presented below.

The following system dynamics can be represented by rewriting the equations above in matrix form as $\{y(t)\} = [C]\{x(t)\} + [B]u(t)$

$$\begin{Bmatrix} y(t)_1 \\ y(t)_2 \\ y(t)_3 \\ y(t)_4 \\ y(t)_5 \\ y(t)_6 \\ y(t)_7 \\ y(t)_8 \\ y(t)_9 \\ y(t)_{10} \\ y(t)_{11} \end{Bmatrix} = \begin{bmatrix} 1\,0\,0\,0\,0\,0\,0\,0\,0\,0\,0\,0\,0\,0\,0\,0\,0\,0\,0\,0\,0 \\ 0\,0\,1\,0\,0\,0\,0\,0\,0\,0\,0\,0\,0\,0\,0\,0\,0\,0\,0\,0\,0 \\ 0\,0\,0\,0\,1\,0\,0\,0\,0\,0\,0\,0\,0\,0\,0\,0\,0\,0\,0\,0\,0 \\ 0\,0\,0\,0\,0\,0\,1\,0\,0\,0\,0\,0\,0\,0\,0\,0\,0\,0\,0\,0\,0 \\ 0\,0\,0\,0\,0\,0\,0\,0\,1\,0\,0\,0\,0\,0\,0\,0\,0\,0\,0\,0\,0 \\ 0\,0\,0\,0\,0\,0\,0\,0\,0\,0\,1\,0\,0\,0\,0\,0\,0\,0\,0\,0\,0 \\ 0\,0\,0\,0\,0\,0\,0\,0\,0\,0\,0\,0\,1\,0\,0\,0\,0\,0\,0\,0\,0 \\ 0\,0\,0\,0\,0\,0\,0\,0\,0\,0\,0\,0\,0\,0\,1\,0\,0\,0\,0\,0\,0 \\ 0\,0\,0\,0\,0\,0\,0\,0\,0\,0\,0\,0\,0\,0\,0\,1\,0\,0\,0\,0\,0 \\ 0\,0\,0\,0\,0\,0\,0\,0\,0\,0\,0\,0\,0\,0\,0\,0\,1\,0\,0\,0\,0 \\ 0\,0\,0\,0\,0\,0\,0\,0\,0\,0\,0\,0\,0\,0\,0\,0\,0\,1\,0\,0\,0 \\ 0\,0\,0\,0\,0\,0\,0\,0\,0\,0\,0\,0\,0\,0\,0\,0\,0\,0\,1\,0\,0 \\ 0\,0\,0\,0\,0\,0\,0\,0\,0\,0\,0\,0\,0\,0\,0\,0\,0\,0\,0\,1\,0 \end{bmatrix} \begin{Bmatrix} x(t)_1 \\ x(t)_2 \\ x(t)_3 \\ x(t)_4 \\ x(t)_5 \\ x(t)_6 \\ x(t)_7 \\ x(t)_8 \\ x(t)_9 \\ x(t)_{10} \\ x(t)_{11} \\ x(t)_{12} \\ x(t)_{13} \\ x(t)_{14} \\ x(t)_{15} \\ x(t)_{16} \\ x(t)_{17} \\ x(t)_{18} \\ x(t)_{19} \\ x(t)_{20} \\ x(t)_{21} \\ x(t)_{22} \end{Bmatrix} + (0)(1) \tag{33}$$

6. **Results and Discussion.** The system's transient response is calculated by solving the coupled linear differential equations from (1)-(13) using Laplace transforms for state space analysis with initial conditions, inverse matrix Laplace and matrix exponential in state space form. The process is detailed in Equations (14)-(33). This allows us to obtain the $y_i(t)$ $(i = 1, 2, \ldots, 11)$ response for all 11 degrees of freedom and solve for the transient response.

6.1. **Validation of the occupant and wheelchair model.** We present a rigorous validation of our 11-DOF wheelchair-occupant model, emphasizing its robustness and accuracy. The validation process is based on a detailed comparison of calculated and experimental acceleration ratios, a crucial aspect for ensuring the reliability of our model. Figure 2 provides a comprehensive view of this comparison. The analysis examines the acceleration ratios of input forces acting on the occupant, ranging from the torso to the pelvis. Remarkably, our investigation reveals that the values of these ratios are situated in the frequency range of 0.5∼11 [Hz] [30]. The stiffness and damping parameters of the foam seat cushion under examination are meticulously documented in Tables 1 and 2. These parameters serve as fundamental input for our composite model, and the resulting acceleration ratios are presented graphically in Figure 2. Notably, the first peak value emerges at a frequency of approximately 3 to 4 [Hz]. To gauge the model's performance, we conduct a comparative analysis against the experimental curve derived by Patil and Palanichamy [30]. The experimental data, acquired from tests involving sinusoidal inputs [30, 36], show a commendable agreement with our model's results. This alignment confirms the acceptability and fidelity of our composite model. Figure 2 showcases the comparison between the calculated and experimental acceleration ratios of the torso to

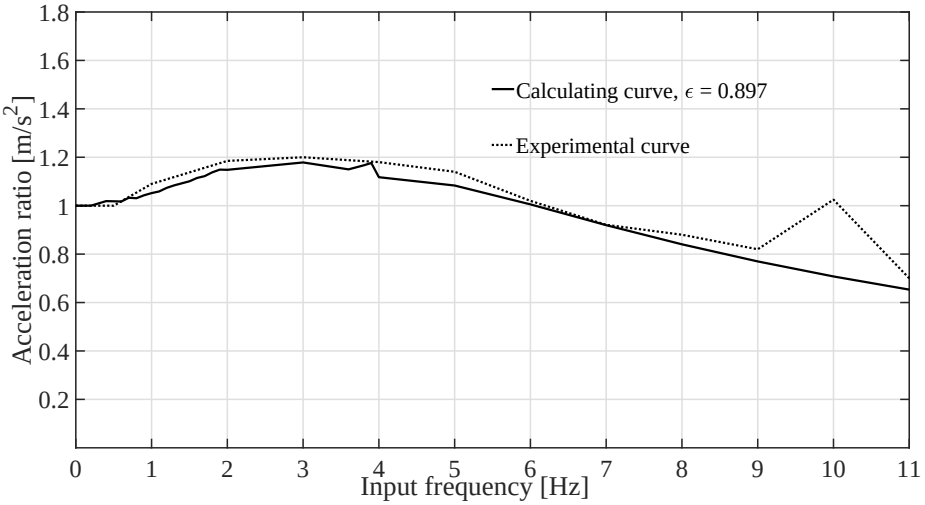

FIGURE 2. Comparison of calculated and experimental acceleration ratios [35] of a wheelchair-occupant on a foam seat cushion

the pelvis, highlighting the model's capacity to faithfully replicate the dynamic behavior of the wheelchair-occupant system under diverse input conditions. The solid line represents the calculated acceleration ratio as a function of input frequency in the range of 0.5∼11 [Hz], while the dashed line corresponds to the experimental data. The exceptional match between the calculated and experimental results is quantified by a goodness-of-fit of 89.7[%], indicating a high level of agreement. This validation not only fortifies the credibility of our 11-DOF model but also accentuates its potential as a valuable tool for understanding and optimizing the dynamic response of wheelchair-occupant systems in real-world scenarios.

6.2. **Transient vibration responses of wheelchair-occupant system with foam-based seat cushion under sinusoidal vibration inputs: A time-domain analysis using state space model and Laplace transform.** Transient vibrations are inevitable phenomena that wheelchair users encounter during their daily activities, such as propelling, braking, and turning. These vibrations can affect the comfort and safety of wheelchair users, depending on their frequency, amplitude, and duration. Therefore, it is essential to understand how different body parts of wheelchair users respond to transient vibrations and what the potential damage thresholds are that should be avoided or minimized. Previous studies have investigated the vibration responses of wheelchair-occupant systems under different conditions, such as road surface, wheelchair tires and seat cushions. However, most of these studies focused on steady-state vibrations, which are constant and periodic, and did not consider the transient nature of vibrations, which are variable and non-periodic. Moreover, most of these studies used numerical or experimental methods, which are limited by computational or practical constraints, and did not provide analytical solutions, which are more general and comprehensive. In this paper, we aim to fill these gaps by examining the transient vibration responses of a wheelchair-occupant system with foam-based seat cushions under sinusoidal vibration inputs, which are commonly used to simulate transient vibrations. We applied a time-domain analysis with a state space model and Laplace transform to obtaining analytical solutions for displacement responses. We validated our model with experimental data and studied the effects of vibrations on the torso and pelvis, which have the largest relative displacements when seated on foam-based cushions. We classified the sinusoidal vibration inputs into

low and high frequencies, based on their characteristics and sources, such as propelling, braking, and turning. We estimated potential damage thresholds based on peak to peak displacement of body parts and evaluated different foam-based cushions, providing useful guidance for choosing the most appropriate cushion for specific applications.

This paper investigated the transient vibration responses of different body parts and the seat of a wheelchair-occupant system subjected to a pulse input. Figures 3-6 show the displacement amplitudes of the head, torso, thorax, abdomen, back, diaphragm, pelvis, and seat over time. The main findings are as follows. The torso experienced the highest displacement amplitude of 0.0174 [mm] at 0.194 seconds, followed by the head with 0.0168 [mm] at the same time point (Figure 3). This indicates that the upper body was more affected by the pulse input than the lower body. The pelvis had the lowest displacement amplitude of 0.0157 [mm] at 0.194 seconds, while the seat had a slightly higher displacement amplitude of 0.0176 [mm] at 0.0645 seconds (Figure 6). This suggests that the pelvis was well supported by the seat and had less relative motion with respect to the wheelchair. The thorax and the abdomen had similar displacement amplitudes, peaking at 0.0173 [mm] and 0.0166 [mm] respectively at 0.21 seconds (Figures 4 and 5). The diaphragm and the back also had almost identical displacement amplitudes, reaching 0.0169 [mm] and 0.0167 [mm] respectively at 0.194 seconds (Figures 3 and 5). This implies that the thorax-abdomen and back-diaphragm combinations had similar stiffness and damping properties and responded similarly to the pulse input. The transient responses of all body parts and the seat gradually decreased and returned to zero within 2.61 seconds. This shows that the system reached a steady state after the pulse input. These results can be explained by the different stiffness and damping properties of the body parts and the foam-based seat cushion, as well as the coupling effects between the body and the wheelchair. The results are consistent with previous studies that have reported the transient vibration responses of the wheelchair-occupant system. The results can also be used to evaluate the performance and comfort of different foam-based seat cushions for wheelchair users. The results can also provide insights for designing and optimizing the wheelchair-occupant system to reduce the adverse effects of vibrations on the human body.

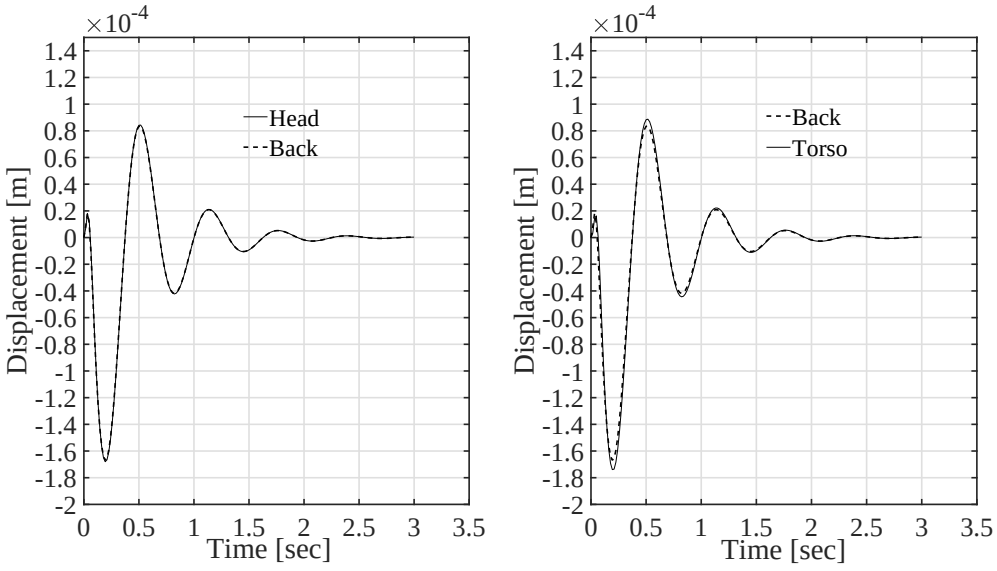

FIGURE 3. Comparing the transient response of the head-back and back-torso to a step input with varying displacement and time

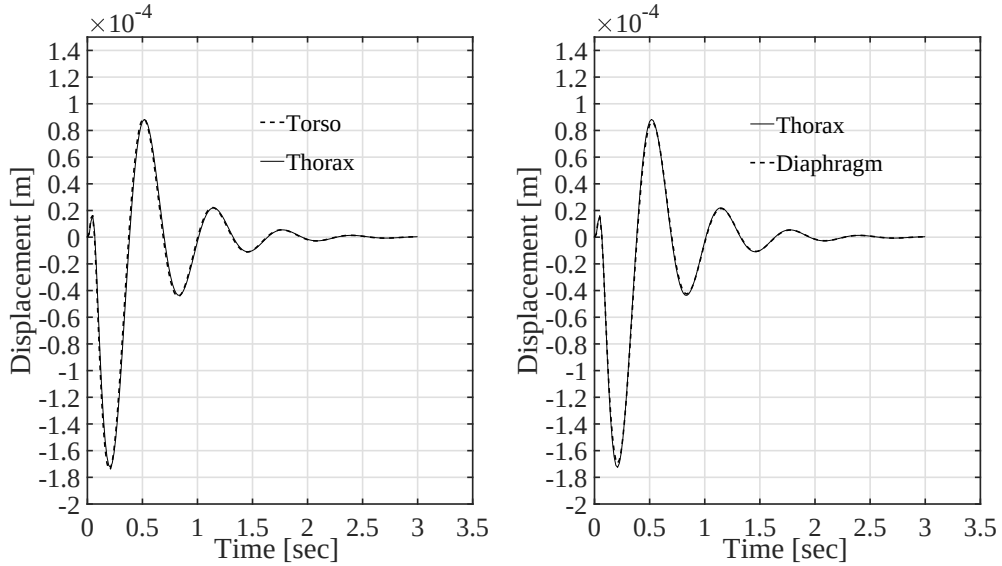

FIGURE 4. Comparing the transient response of the torso-thorax and thorax-diaphragm to a step input with varying displacement and time

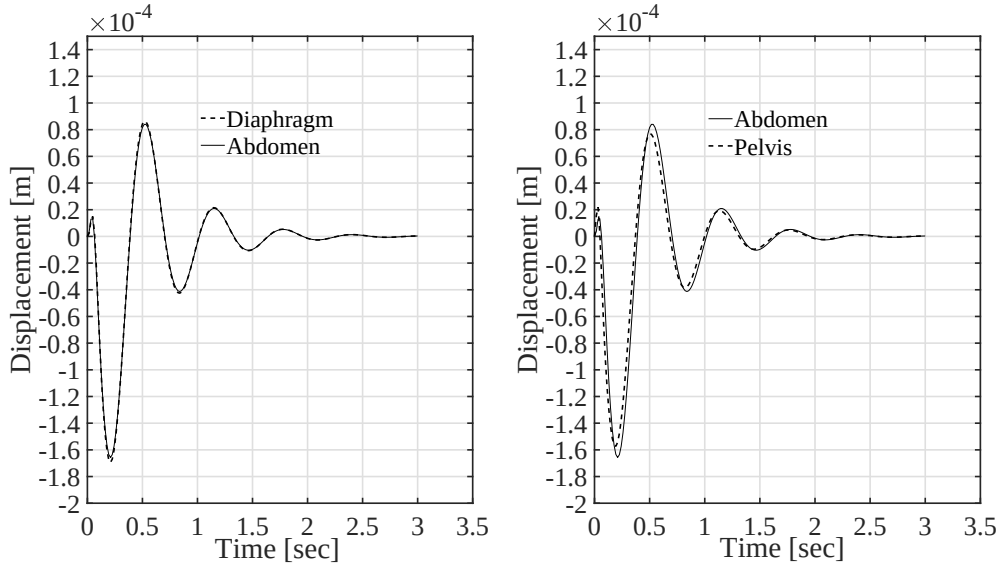

FIGURE 5. Comparing the transient response of the diaphragm-abdomen and abdomen-pelvis to a step input with varying displacement and time

Figures 3-6 show the transient responses of various body part combinations, including the head, back, torso, thorax, abdomen, diaphragm and pelvis, to sinusoidal vibration inputs with different frequencies and amplitudes. The figure shows the relative amplitude, frequency, and time of the maximum and minimum values for each body part combination. The figure also shows the input vibration applied to the tires and the seat. We can also observe that the responses of different body part combinations had different characteristics, depending on the frequency and amplitude of the input vibration. For example, the head-back response had a low amplitude and a low frequency, while the pelvis-back response had a high amplitude and a high frequency. These observations suggest that the body and the wheelchair have different natural frequencies and damping ratios, which affect their vibration modes and energy dissipation.

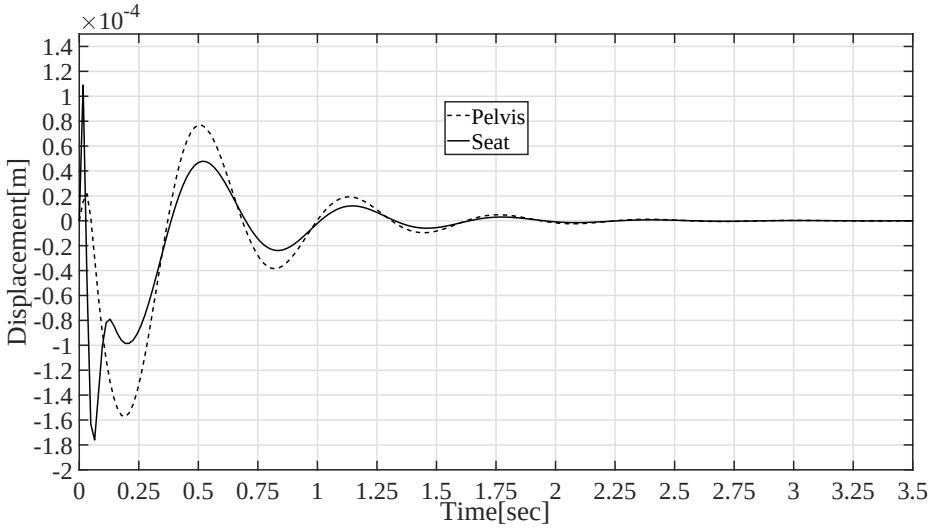

FIGURE 6. Comparing the transient response of the pelvis-back and seat to a step input with varying displacement and time

To further compare the responses of different body segments and wheelchair components, we summarized the results of Figures 3-6 in Table 3, which presents the comparison of transient maximum responses of body and wheelchair parts relative to adjacent body parts under sinusoidal vibration inputs. The table shows the relative amplitude, frequency, and time of the maximum response for each body part. The relative amplitude measures the displacement difference between the current and adjacent masses, indicating the degree of vibration transmission. The frequency measures the vibration cycles per second, reflecting the resonance characteristics. The time measures when the maximum relative amplitude occurs, showing the delay.

TABLE 3. Comparison of transient maximum responses of body and wheelchair parts

The amplitude relative to adjacent body parts				
Mass	Relative amplitude [mm]	Frequency [Hz]	Time [s]	Body parts
Head	0.0023	1.53	0.065	Head-Back
Back	0.0149	2.34	0.0806	Back-Torso
Torso	0.0096	4.83	0.113	Torso-Thorax
Thorax	0.0042	6.18	0.161	Thorax-Diaphragm
Diaphragm	0.0039	8.86	0.194	Diaphragm-Abdomen
Abdomen	0.0368	10.52	0.0806	Abdomen-Pelvis
Pelvis	0.0196	12.87	0.0806	Pelvis-Back

From Table 3, we can observe the following. i) Abdomen and back are the most vulnerable body parts to vibrations. The abdomen has the highest relative amplitude of 0.0368 [mm], followed by the pelvis with 0.0196 [mm]. The high relative amplitude of the abdomen may be due to its soft tissue and low stiffness, which makes it more susceptible to vibration. These findings suggest that the abdomen and the pelvis need more protection and cushioning from vibrations [36, 37]. ii) Head is the most stable body part. The head has the lowest relative amplitude of 0.0023 [mm]. The low relative amplitude of the head may be due to its high stiffness and damping, which makes it more resistant to vibration

[31, 32]. These findings imply that the head is less affected by vibrations and does not require much attention. iii) Frequency of the maximum response increases from head to pelvis. The frequency of the maximum response ranges from 1.53 [Hz] for the head to 12.87 [Hz] for the pelvis. This may be explained by the fact that the lower body parts have lower natural frequencies than the upper body parts, and thus they resonate more with the higher frequency components of the input vibration [36, 37]. These results indicate that the lower body parts are more sensitive to vibrations and need more damping and isolation. iv) Diaphragm has the largest phase lag with respect to the input vibration. The diaphragm has the longest time of 0.194 seconds, in contrast, the head has the shortest recorded duration of 0.065 seconds. These results show that the diaphragm has the largest phase difference with the input vibration, which may affect its function and performance [30, 31]. These results suggest that the diaphragm needs more synchronization and control.

One of the main goals of this study was to evaluate the safety and integrity of the body during transient vibration events, which can cause damage or injury to the body tissues. To do this, we estimated the strain value based on the length change between the abdomen and pelvis, as suggested by previous studies. The strain value represents the deformation of the body tissues due to the vibration-induced displacement. We found that the strain value was 5.7[%], which was much lower than the critical strain percentage or breaking index (42[%]) for the same body parts reported by Patil and Palanichamy [30]. This indicates that the strain levels were well within the safe limits and did not pose any risk of damage or injury to the body tissues. These findings confirm the validity and reliability of our analytical model and experimental data.

7. **Conclusions.** This paper developed and validated a 11-DOF model of a wheelchair-occupant system with foam-based seat cushions under sinusoidal vibration inputs. The model was able to capture the transient vibration responses of different body parts and the seat, and to compare them with experimental data. The results revealed that the torso experienced the highest acceleration ratio, indicating the highest degree of vibration transmission, while the pelvis experienced the lowest acceleration ratio, indicating the lowest degree of vibration transmission. The model also showed a high level of agreement with the experimental data, with a goodness-of-fit of 89.7[%]. These findings have important implications for evaluating and improving the comfort and safety of wheelchair users under transient vibration events. They also provide useful guidance for designing systems that meet the specific needs and preferences of wheelchair users and enhance their quality of life. This paper is the first to investigate the transient vibration responses of a wheelchair-occupant system with foam-based seat cushions under sinusoidal inputs. It adds to the existing knowledge base for the selection and use of these cushions in various applications. It also opens up new avenues for future research on the vibration behavior of wheelchair-occupant systems, such as exploring different seating configurations, cushion materials and suspension systems within the 11-DOF model, considering other factors such as road surface conditions, wheel types and environmental factors, conducting user studies and collecting feedback on the proposed seat cushion designs and investigating the transmissibility behavior of seating systems and cushions, along with different input vibrations.

Acknowledgment. This material is the result of work supported by JSPS KAKENHI Grant Number JP21K03930.

REFERENCES

[1] Y. Garcia-Mendez, J. L. Pearlman, M. L. Boninger and R. A. Cooper, Health risks of vibration exposure to wheelchair users in the community, *The Journal of Spinal Cord Medicine*, vol.36, no.4, pp.365-375, 2013.

[2] O. Lariviere, D. Chadefaux, C. Sauret and P. Thoreux, Vibration transmission during manual wheelchair propulsion: A systematic review, *Vibration*, vol.4, pp.444-481, 2021.

[3] J. L. Candiotti, A. Neti, S. Sivakanthan and R. A. Cooper, Analysis of whole-body vibration using electric powered wheelchairs on surface transitions, *Vibration*, vol.5, no.1, pp.98-109, 2022.

[4] M. M. Alipour, Transient forced vibration response analysis of heterogeneous sandwich circular plates under viscoelastic boundary support, *Archives of Civil and Mechanical Engineering*, vol.18, no.1, pp.12-31, 2018.

[5] E. Wolf, R. A. Cooper, J. Pearlman, S. G. Fitzgerald and A. Kelleher, Longitudinal assessment of vibrations during manual and power wheelchair driving over select sidewalk surfaces, *Journal of Rehabilitation Research & Development*, vol.44, no.4, pp.573-580, 2007.

[6] B. A. Gordeev, S. N. Okhulkov, A. N. Osmekhin and A. E. Shokhin, Reducing transient vibrations due to rotating shafts, *Russian Engineering Research*, vol.38, no.5, pp.335-341, 2018.

[7] J. Wang and C. M. Mak, An indicator for the assessment of isolation performance of transient vibration, *Journal of Vibration & Control*, vol.19, no.16, pp.1479-1490, 2012.

[8] C. He and P. Shi, Interface pressure reduction effects of wheelchair cushions in individuals with spinal cord injury: A rapid review, *Disability and Rehabilitation*, vol.44, no.6, pp.827-834, 2022.

[9] K. D. Klinich, M. A. Manary, N. R. Orton, K. Boyle and J. Hu, A literature review of wheelchair transportation safety relevant to automated vehicles, *International Journal of Environmental Research & Public Health*, vol.19, no.3, pp.1-19, 2022.

[10] E. Wolf, J. Pearlman, M. L. Boninger and R. A. Cooper, Health risks of vibration exposure to wheelchair users in the community, *The Journal of Spinal Cord Medicine*, vol.31, no.4, pp.361-369, 2008.

[11] M. AlShabi, W. Araydah, H. ElShatarat, M. Othman, M. B. Younis and S. A. Gadsden, Effect of mechanical vibrations on the human body, *World Journal of Mechanics*, vol.6, no.9, pp.273-304, 2016.

[12] D. P. VanSickle, R. A. Cooper, M. L. Boninger and C. P. DiGiovine, Analysis of vibrations induced during wheelchair propulsion, *Journal of Rehabilitation Research & Development*, vol.38, no.4, pp.409-421, 2001.

[13] H. E. Veeger, L. H. van der Woude and R. H. Rozendal, Effect of handrim velocity on mechanical efficiency in wheelchair propulsion, *Medicine & Science in Sports & Exercise*, vol.24, no.1, pp.100-107, 1992.

[14] S. N. W. Vorrink, L. H. V. Van der Woude, A. Messenberg, P. A. Cripton, B. Hughes and B. J. Sawatzky, Comparison of wheelchair wheels in terms of vibration and spasticity in people with spinal cord injury, *Journal of Rehabilitation Research & Development*, vol.45, pp.1269-1280, 2008.

[15] T. Waga, S. Ura, M. Nagamori, H. Uchiyama and A. Shionoya, Influence of material on wheelchair vibrations, *Proceedings*, vol.49, pp.1-13, 2020.

[16] A. Faupin, P. Campillo, T. Weissland, P. Gorce and A. Thevenon, The effects of rear-wheel camber on the mechanical parameters produced during the wheelchair sprinting of handibasketball athletes, *Journal of Rehabilitation Research & Development*, vol.41, no.3B, pp.421-428, 2004.

[17] F. Chénier and R. Aissaoui, Effect of wheelchair frame material on users' mechanical work and transmitted vibration, *Biomedical Research*, vol.2014, pp.1-12, 2014.

[18] H. T. Bui, Q. B. Tao, P. Lestriez, K. Debray and V. T. Hoang, Evaluation of temperature on different wheelchair cushions using infrared thermography method, *Journal of Mechanical Science & Technology*, vol.37, pp.1-8, 2023.

[19] Y. Garcia-Mendez, J. L. Pearlman, R. A. Cooper and M. L. Boninger, Dynamic stiffness and transmissibility of commercially available wheelchair cushions using a laboratory test method, *Journal of Rehabilitation Research & Development*, vol.49, no.1, pp.7-22, 2012.

[20] M. Ferguson-Pell, G. Ferguson-Pell, F. Mohammadi and E. Call, Applying ISO 16840-2 Standard to differentiate impact force dissipation characteristics of selection of commercial wheelchair cushions, *Journal of Rehabilitation Research & Development*, vol.52, pp.41-52, 2015.

[21] P. Weerapong, K. Hashikura, M. A. S. Kamal, I. Murakam and K. Yamada, Simulated response analysis: Modelling a wheelchair occupant system subjected to vibration, *International Journal of Innovative Computing, Information and Control*, vol.19, no.2, pp.307-323, 2023.

[22] P. Weerapong, K. Hashikura, M. A. S. Kamal, I. Murakam and K. Yamada, Analysis of model output in the simulation of a wheelchair-occupant system subjected to vibration, *ICIC Express Letters, Part B: Applications*, vol.14, no.4, pp.389-398, 2023.
[23] J. Misch and S. Sprigle, Estimating whole-body vibration limits of manual wheelchair mobility over common surfaces, *Journal of Rehabilitation and Assistive Technologies Engineering*, vol.9, pp.1-5, 2022.
[24] Y. Garcia-Mendez, J. Pearlman and R. A. Cooper, Vibration exposure in wheelchairs: The effect of pressure and tire type, *Assist. Technol.*, vol.32, no.1, pp.1-8, 2020.
[25] P. Weerapong, K. Hashikura, M. A. S. Kamal and K. Yamada, A model for the response of an occupant and wheelchair system subjected to vertical vibrations, *International Journal of Innovative Computing, Information and Control*, vol.17, no.6, pp.1823-1841, 2021.
[26] P. Weerapong, K. Hashikura, M. A. S. Kamal and K. Yamada, A biodynamic model of wheelchair with changeable seat cushions subjected to vertical vibrations, *ICIC Express Letters*, vol.16, no.1, pp.33-41, 2022.
[27] S. Badran, A. Salah, W. Abbas and O. B. Abouelatta, Optimal linear suspension design for quarter car with human model using genetic algorithms, *The Research Bulletin of Jordan ACM*, vol.2, no.2, pp.42-51, 2012.
[28] R. Solea and U. Nunes, Robotic wheelchair control considering user comfort: Modeling and experimental evaluation, *Informatics in Control, Automation & Robotics*, vol.37, pp.113-125, 2008.
[29] J. Duvall, E. Sinagra, R. Cooper and J. Pearlman, Pedestrian pathway roughness thresholds for wheelchair users' safety and comfort, *Assist. Technol.*, vol.28, no.4, pp.209-215, 2016.
[30] M. K. Patil and M. S. Palanichamy, A mathematical model of tractor-occupant system with a new seat suspension for minimization of vibration response, *Applied Mathematical Modelling*, vol.12, pp.63-71, 1988.
[31] C. C. Liang and C. F. Chiang, A study on biodynamic models of seated human subjects exposed to vertical vibration, *International Journal of Industrial Ergonomics*, vol.36, pp.869-890, 2006.
[32] M. F. Hikmawan and A. S. Nugraha, Analysis of electric wheelchair passenger comfort with a half car model approach, *International Conference on Sustainable Energy Engineering & Application (ICSEEA 2016)*, pp.76-80, 2016.
[33] M. B. Parkinson and C. J. Garneau, State space analysis of seat cushion dynamic response, *Journal of Sound & Vibration*, vol.330, pp.4471-4483, 2011.
[34] M. R. Hatch, *Vibration Simulation Using MATLAB & ANSYS*, Chapman and Hall/CRC, New York, 2001.
[35] M. S. Palanichamy, M. K. Patil and D. N. Ghista, Minimization of the vertical vibrations sustained by tractor operator, by provision of a standard-type tractor seat suspension, *Annals of Biomedical Engineering*, vol.5, pp.138-153, 1978.
[36] T. Yoshimura, K. Nakai and G. Tamaoki, Multi-body dynamics modelling of seated human body under exposure to whole-body vibration, *Industrial Health*, vol.43, pp.441-447, 2005.
[37] J. D. Quadros, P. Suhas and N. L. Vaishak, A numerical study for determining the ideal operating speed for a two-wheeler rider on varying terrain amplitudes, *Journal of Mechanical Science & Technology*, vol.30, pp.2435-2442, 2016.

Author Biography

Pongtep Weerapong received his B.E. and M.E. degrees in Materials Engineering and Polymer Processing Engineering, respectively, from King Mongkut's University of Technology Thonburi (KMUTT), Thailand. He obtained his Ph.D. degree from Gunma University, Japan, in 2023. He is currently a full-time professor at the Faculty of Industrial Technology at Nakhon Si Thammarat Rajabhat University, Thailand. His current research interests include assistive technology for children with disabilities and whole-body vibration.

Kreetha Kaewkongtham received the B.E. degree in Materials Handling Technology in 2000 and the B.Ind.Tech degree in Mechanical Technology in 2009 from King Mongkut's University of Technology North Bangkok (KMUTNB), Thailand. He is currently a full-time professor at the Faculty of Industrial Technology at Nakhon Si Thammarat Rajabhat University, Thailand. His research interests include assistive technology, pneumatic systems and whole-body vibration.

Narapong Chuaychai received the B.Ind.Tech degree in Welding Technology from King Mongkut's University of Technology North Bangkok, Thailand, in 2000. He obtained the Master of Education (Industrial Technology) from Nakhon Si Thammarat Rajabhat University, Thailand, in 2012 and his Ph.D. degree from Phranakhon Rajabhat University, Thailand, in 2019. He is currently a full-time professor at the Faculty of Industrial Technology at Nakhon Si Thammarat Rajabhat University, Thailand. His research interests include welding technology, assistive technology and whole-body vibration.

Chatchai Kaewdee received the B.F.A. degree and M.A. degree in Ceramics Program from Silpakorn University, Thailand and his Ph.D. degree in Product Design from Ubon Ratchathani University, Thailand. He is currently a full-time professor of Faculty of Industrial Technology at Nakhon Si Thammarat Rajabhat University, Thailand. His research interests include ceramic product design, mass production of ceramics, direct marketing and influencing ceramic consumers.

Weerayute Sudsomboon is a mechanical engineer and an educator with a passion for learning innovation and technology. He earned a B.S.Ind.Ed. in Mechanical Engineering from King Mongkut's University of Technology Thonburi (KMUTT), an M.Ind.Ed. in Vocational Education Administration from King Mongkut's Institute of Technology Ladkrabang (KMITL) and a Ph.D. degree in Learning Innovation in Technology from KMUTT. His research interests include modern automotive technology education, mechanical engineering education, mechanical system and signal processing, appropriate technology for community and rural settings and vocational and technical education administration and whole-body vibration.

Weeraphol Pansrinual received the B.Sc. degree in Industrial Technology (Electronics) from Rajabhat Institute Phanakhonsriayuttaya and M.Ed. degree in Industrial Technology (Electronics) and Ph.D. degree in Technology Management from Phranakhon Rajabhat University, Thailand, in 2010. He is currently a full-time professor of Faculty of Industrial Technology at Nakhon Si Thammarat Rajabhat University, Thailand. His research interests include mechanical engineering education and vocational and technical education administration.

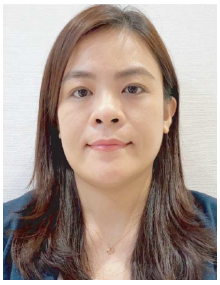

Nghia Thi Mai received the B.S., M.S. and Dr. Eng. degrees from Gunma University, Gunma, Japan in 2009, 2011 and 2014, respectively. From 2014 to 2015, she was with the Human Resources Cultivation Center, Gunma University, Gunma, Japan as a research associate. From 2015 to 2021, she worked on research on damping control for automobiles at Exedy Co., Ltd. Since 2022, she has been working as a lecturer at the Department of Electrical and Electronic 1, Posts and Telecommunications Institute of Technology (PTIT). In addition, she is currently working as a visiting associate professor and part-time lecturer at the Department of Electronics and Mechanical Engineering, Gunma University. Her research interest includes Smith predictor, internal model control and robotics.

Mitsuki Katahira received the B.E. degree in Mechanical Science and Technology from Gunma University, Japan in 2022. He is now a master course student at Gunma University, Japan. His research interests include assistive technology for children with disabilities and whole-body vibration.

Kotaro Hashikura received the B.S. degree in Mechanical Engineering from Kyushu Institute of Technology, Fukuoka, Japan, 2006; the M.S. degree of Informatics from Kyoto University, Kyoto, Japan 2010; and the Doctor degree in Engineering from Tokyo Metropolitan University, Tokyo, Japan, 2014. From 2014 until 2018, he had been a Project Research Associate at the Faculty of System Design, Tokyo Metropolitan University. He is currently a full-time professor at Division of Mechanical Science and Technology, Gunma University, Japan. His research interests include time-delay-related control techniques, such as deadbeat, preview-prediction and repetitive controls. He is a member of IEEE, ISCIE and SICE.

Md Abdus Samad Kamal received the B.Sc. degree in Electrical and Electronic Engineering from Khulna University of Engineering and Technology (KUET), Khulna, Bangladesh in 1997; Master and Doctor degrees from Kyushu University from Graduate School of Information Science and Electrical Engineering, Japan in 2003 and 2006, respectively. He was a post-doctoral fellow in Kyushu University till November 2006. He is currently a full-time professor at Division of Mechanical Science and Technology, Gunma University, Japan. His current research interests include reinforcement learning, intelligent transportation systems and multiagent systems. He is a member of IEEE and SICE.

Iwanori Murakami received the B.E., M.E. and Dr. Eng. degrees from Gunma University, Kiryu City, Japan, in 1992, 1994 and 1997, respectively. He is currently a full-time professor at Division of Mechanical Science and Technology, Gunma University, Japan. His research interests include control problems in the mechanical fields and robotics.

Kou Yamada received B.S. and M.S. degrees in Electrical and Information Engineering from Yamagata University, Yamagata, Japan, 1987 and 1989, respectively; and the Dr. Eng. Degree from Osaka University, Osaka, Japan in 1997. He is currently a full-time professor at Division of Mechanical Science and Technology, Gunma University, Japan. His research interests include robust control, repetitive control, process control and control theory for inverse systems and infinite-dimensional systems. Prof. Yamada received the 2005 Yokoyama Award in Science and Technology, the 2005 Electrical Engineering/Electronics, Computer, Telecommunication and Information Technology International Conference (ECTI-CON2005) Best Paper Award, the Japanese Ergonomics Society Encouragement Award for Academic Paper in 2007, the 2008 Electrical Engineering/Electronics, Computer, Telecommunication and Information Technology International Conference (ECTI-CON2008) Best Paper Award and 4th International Conference on Innovative Computing, Information and Control Best Paper Award in 2009, the 14th International Conference on Innovative Computing, Information and Control Best Paper Award in 2019, Outstanding Achievement Award from Kanto Branch of Japanese Society for Engineering Education in 2022 and JSME (The Japan Society of Mechanical Engineers) Education Award in 2023. He is a member of IEEE and SICE and a fellow of JSME.